

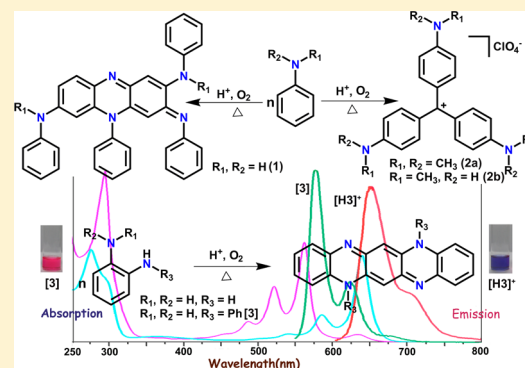
Aerial Oxidation of Protonated Aromatic Amines. Isolation, X-ray Structure, and Redox and Spectral Characteristics of N-Containing Dyes

Suman K Roy, Subhas Samanta, Mominul Sinan, Pradip Ghosh, and Sreebrata Goswami*

Department of Inorganic Chemistry, Indian Association for the Cultivation of Science, Kolkata 700 032, India

S Supporting Information

ABSTRACT: This work reports the results of our investigation on the aerial oxidation of aromatic amines that are promoted by protic acid. While primary aromatic amines produce substituted phenazines as major products, *N*-phenyl-*o*-phenylenediamine produces polycyclic aromatic heterocycles like azaacene and secondary and tertiary amines give exclusively the dyes containing a triphenylmethane moiety. Isolation of the compounds and the effects of substitutions on the aromatic rings have been investigated. In this context, plausible reaction steps that are involved have been discussed. Single-crystal X-ray structure analyses of the representative compounds are solved to authenticate their formation. In almost every case, a high degree of delocalization of electron was noted. The compounds have been characterized thoroughly and show rich spectral properties. For example, the phenazine molecules exhibited absorption peaks between 475 and 605 nm because of the charge-transfer transition from the amine and tricyclopopyrazine moiety. Their acidochromic and solvatochromic behaviors, which are supported by theoretical calculations, are investigated. The polycyclic azacene molecule exhibits strong absorption in the visible region and fluoresces with high quantum yield. The phenazine dyes undergo a quasi-reversible reduction at a low cathodic potential that varies linearly as a function of Hammett's constant.



INTRODUCTION

Oxidation of aniline is a versatile and valued chemical reaction that has led to the synthesis of many useful organic compounds. Upon oxidation, aniline usually produces nitroso or nitro derivatives. It is also known that oxidative N,N bond fusion reaction of primary aromatic amines leads to formation of hydrazo/azo/azoxy¹ compounds. In contrast, similar oxidation reactions involving carbon–nitrogen bond formation^{2a–f} are poorly developed. It is one of the most important areas of contemporary research because such reactions can produce a variety of nitrogen-containing, high-value chemicals ranging from medicines to functional materials.^{3a–c} Polyaniline is one such prominent example of a chemical that is of paramount importance⁴ in material science.

In recent years, we have been interested in transition-metal-promoted^{5a–k} carbon–nitrogen bond fusion reactions of aniline or its derivatives. It has been established that coordinatively unsaturated metal mediators containing oxidizable metal centers can act as excellent mediators for C_{arom}–N bond-making reactions in anilido substrates.^{5a–k,6a–c} For example, Ru³⁺ and Os⁴⁺ metal ions mediate *ortho*-dimerization of primary aromatic amines (ArNH₂), whereas Fe³⁺ mediates^{5d} multiple C–N bond fusion reactions leading to the formation of phenazine in 4-methoxyaniline. Very recently, we have shown^{5j} that strongly oxidizing OsO₄ can bring about multiple *ortho*-C_{arom}–N bond formation reactions in aniline. All of these

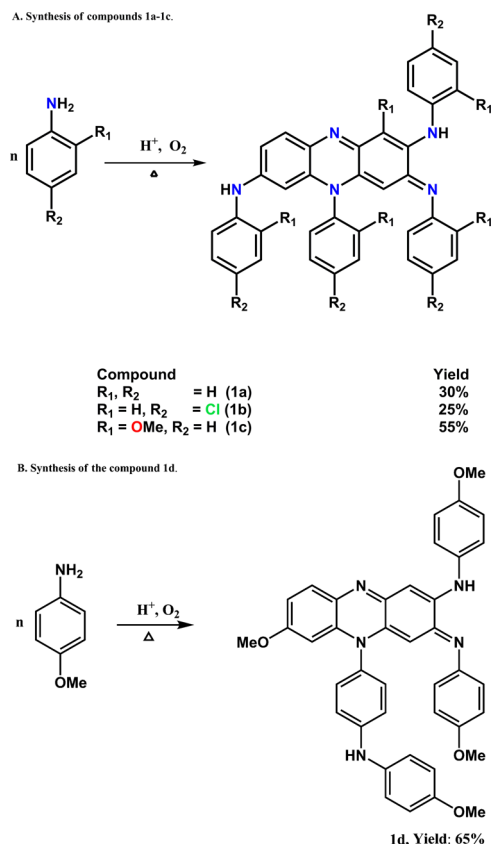
reactions occur under neat conditions and are brought about by air. It has also been established that the mediator transition metal ions, in the above reactions, not only hold anilido substrates in suitable proximity but also directly take part in the redox events.

With this background, we set out to explore the aerial oxidation of protonated aniline substrates in neat solution. Though H⁺ is known to behave as an oxidizing agent,⁷ it cannot act as a template for gathering aniline moieties as it happens with the transition-metal ion mediators. Thus, a different reactivity pattern was anticipated. Accordingly, some chosen protonated anilido substrates heated separately at 373 K in air which resulted in slow color changes. In the cases of primary aromatic amines, substituted phenazines (**1a–d**) were isolated. This chemical transformation is a case of aerial oxidation reaction associated with multiple C_{arom}–N bond formations. In contrast, a secondary aromatic amine like *N*-methylaniline or a tertiary aromatic amine like *N,N*-dimethylaniline followed totally different courses of reactions and yielded highly colored triphenylmethane dyes **2a** and **2b** of the corresponding amines. These chemical transformations are collected in Scheme 1. Furthermore, similar chemical reactions of *N*-phenyl-*o*-phenylenediamine resulted in an azaacene-like polycyclic heterocycle

Received: September 4, 2012

Published: October 18, 2012

Scheme 1. Synthesis of Compounds 1a–d



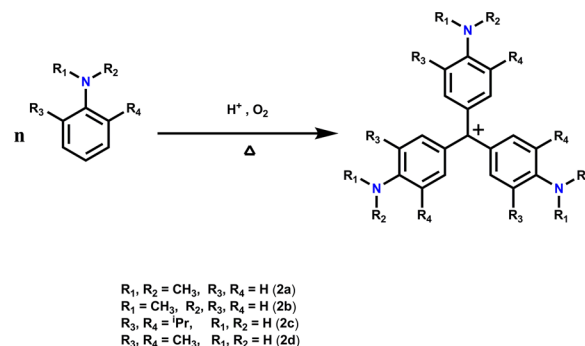
3. Though oxidation of aniline has long been studied, as far as we are aware, proton-assisted oxidation of aniline and its derivatives has not been explored systematically. The reactions, reported herein, have shown some patterns, and many of the products, obtained thereof, are not achievable following conventional synthetic protocols.

RESULTS AND DISCUSSION

Chemical Reactions. Since we are interested in *ortho*-C–N bond fusion reaction of aromatic amines, we purposefully chose aromatic amines without any *ortho*-substitution. When a mixture of 1 g of aniline and 1 M HClO_4 was heated at 100 °C in air, the initial light yellow solution slowly turned brown over 72 h. After the reaction mixture was cooled to room temperature, repeated rapid crystallization from diethyl ether resulted in a brown product. The crude mixture was then loaded on a preparative silica gel TLC plate for purification and on elution by chloroform to afford the phenazine 1a in 30% yield. The reactions also occur with other mineral acids like H_2SO_4 and HCl. However, the reactions are more facile in HClO_4 . Similar reactions with different substituted aromatic anilines were performed, and the products are shown in Scheme 1. In the case of *p*-anisidine, a different positional isomer of the corresponding phenazine compound was obtained.

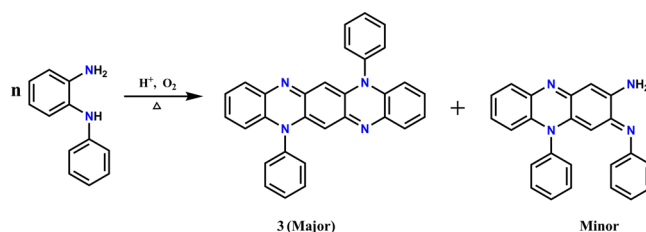
The reactions of secondary and tertiary amines, however, followed different courses and led to the formation of triphenylmethane dyes (Scheme 2). Accordingly, the reaction of *N*-phenyl-*o*-phenylenediamine under similar reaction conditions resulted in the formation of an azaacene-like

Scheme 2. Synthesis of the Triphenylmethane Dyes 2a–d



heterocyclic compound 3 as the major product. The schematic presentation of the reaction is shown in Scheme 3.

Scheme 3. Synthesis of the Compound 3



Experimental details of the above chemical reactions are available as Supporting Information. Microanalytical, positive-ion electron spray ionization mass spectra (ESI-MS), together with NMR spectral data of compounds 1a–e, 2a–d, and 3, convincingly support their formulations. Characterization data of the products are available as Supporting Information (Figures S1–S23). ^1H NMR signals of most of the compounds are generally overlapping, so unambiguous assignment of individual proton signals was not possible. However, proton counts in the spectrum of each of the compounds corroborated with the formulation of products. The characteristic N–H proton signals appeared in the region 8.63–4.53 ppm. For example, compound 1a showed two N–H signals at 5.92 and 8.35 ppm. The crystal violet dyes (2b–d) are symmetric and showed only one N–H signal in the range 4.71–6.74 ppm. ^1H and ^{13}C NMR data of all of the compounds are included in the Experimental Section.

The complexes were primarily characterized by the determination single-crystal X-ray structure analysis of the representative compounds 1a, 1b, 1d, 1e, $[\text{2b}]\text{ClO}_4$, and $[\text{H3}]\text{CF}_3\text{SO}_3$. Suitable crystals of 1a,b,d,e were obtained by slow evaporation of the solution of the respective compound in dichloromethane–hexane mixture. Crystals of $[\text{2b}]\text{ClO}_4$ were obtained by slow diffusion of dichloromethane solution into hexane, and an X-ray quality crystal of the protonated salt $[\text{H3}]\text{CF}_3\text{SO}_3$ was obtained by slow evaporation of its solution in dichloromethane–hexane solvent mixture. Molecular views of compounds 1a and 1d are shown in Figure 1, and those of compounds $[\text{2b}]\text{ClO}_4$ and $[\text{H3}]\text{CF}_3\text{SO}_3$ are shown in Figure 2. A close examination of the bond angles and lengths of the compounds 1a,b,d,e reveals that there has been delocalization of electron in the tricyclo rings [C16–C17–C18–N1–C1–C2–C3–C4–C5–C6–N2–C13–C14–C15]. However the bond parameters of the ring C1–C6 with average C–C length of 1.395 Å are very similar to a benzenoid structure. The

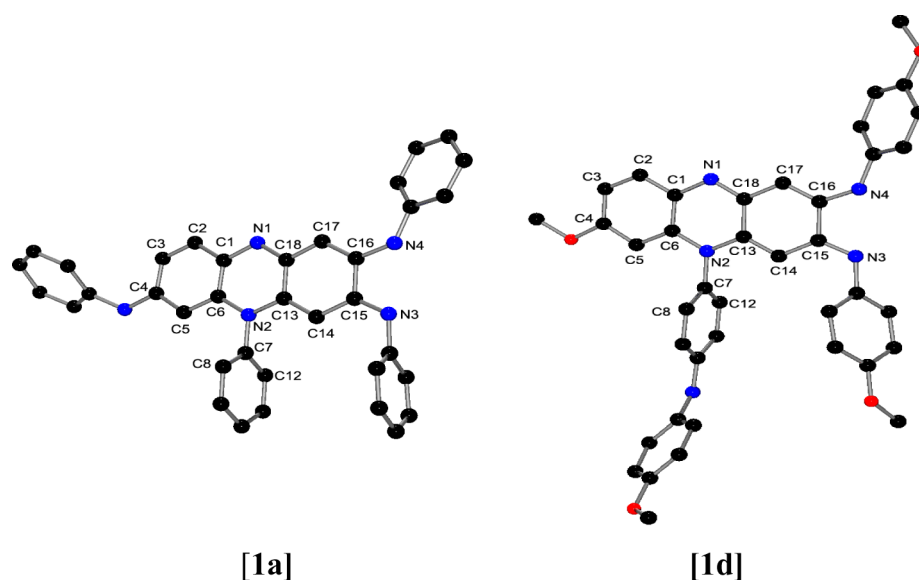
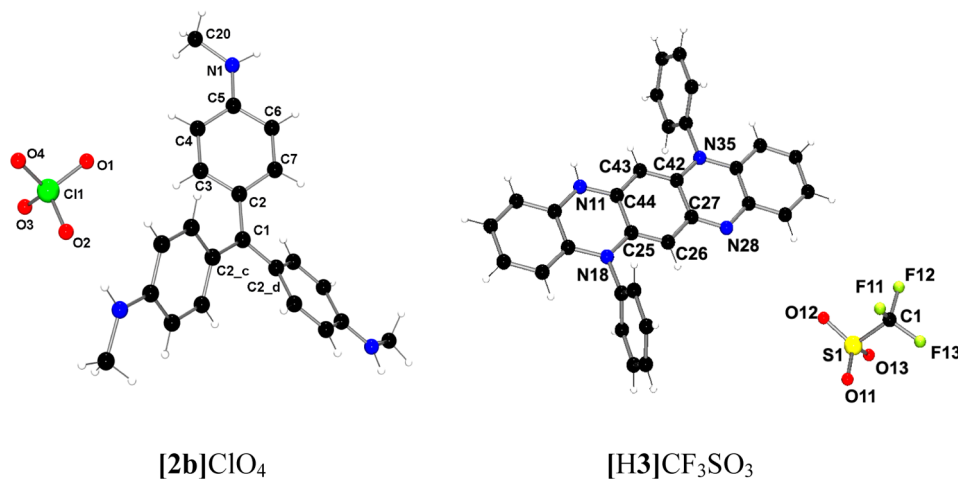


Figure 1. Molecular views of 1a and 1d.

Figure 2. Molecular view of [2b]ClO₄ and [H3]CF₃SO₃.

corresponding bond lengths in the other two rings considerably deviate from benzenoid situation and are more close to a quinonoid form. A least-squares plane calculated through the above 14 atoms of the dibenzo pyrazine fragment indicates that the skeleton is planar with no atom deviating by more than 0.038 Å from the respective plane.

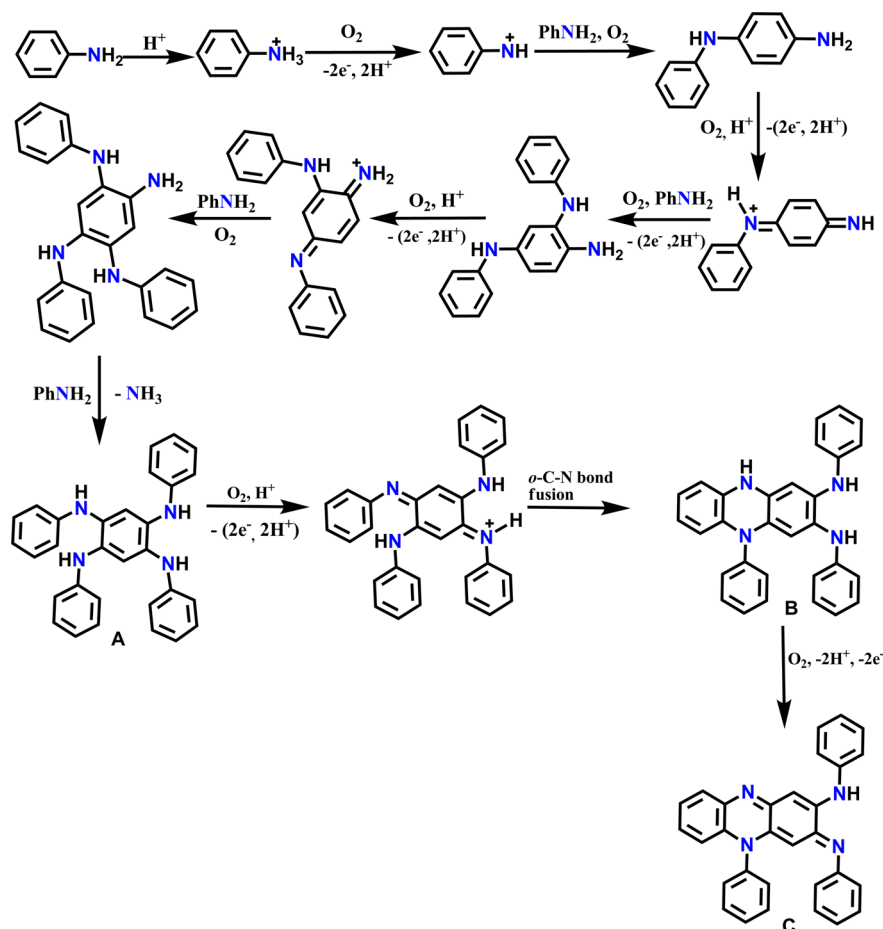
Overall structure solutions have authenticated the formulation of the compounds as shown in Schemes 1–3. Bond parameters of these compounds indicated substantial contributions of the possible resonance forms of the molecules. Furthermore, the middle aryl amine ring in those compounds is nearly perpendicular to the pyrazine ring with a torsional angle C13–N2–C7–C12 = 92.8°. This orientation minimizes the steric interaction between *ortho*-hydrogen *viz* H8 and H12 and those on the phenazine, H5 and H14.

The compound [2b]ClO₄ exists as a symmetric discrete unit. The C–C bond distance between the central carbon atom C1 and the three phenyl rings [(C2, C2_c, C2_d)] is 1.455(6) Å, and the bond distance between the phenyl ring carbon and nitrogen atom of the *N*-methyl group is C5–N1 = 1.346(5) Å. The bond angle between the central carbon(C1) atom and the

two-phenyl carbon atom[(C2_c and C2_d)] is 120°, which confirms that the central carbon atom is sp²-hybridized.

X-ray structure analysis of [H3]CF₃SO₃ has revealed that phenyl substituents are nearly perpendicular to the slightly twisted hexaazapentacene plane. Systematic shortening and lengthening of bond lengths C27–N28 = 1.322 (3) Å and C44–N11 = 1.349 (5) Å and C42–C43 = 1.383 (4) Å, C25–C26 = 1.359 (6) Å clearly indicate a quinonoid structure of the central pyrazine core. However, the two terminal phenyl rings are in perfect benzenoid form (Table 3).

A very limited number of azapentacene compounds have been reported so far and were synthesized using a totally different synthetic protocol than ours. Following an identical synthesis, as described above, we have also isolated unsubstituted azapentacene^{8a–d} (5,12-dihydro-tetraazapentacene 3a) from 1,2-diaminobenzene. ESI-MS and UV–vis spectra of the isolated compound are identical to the reported spectra (see S12 and S41 in the Supporting Information). Furthermore, we note that azapentacenes are important materials and their properties depend on substitution(s) as well. However, to the best of our knowledge, the single-crystal

Scheme 4. Plausible Mechanism of Phenazine by Aerial Oxidation of $[\text{ArNH}_3]^+$ 

X-ray structure of this class of compounds is scarce in the literature.⁹

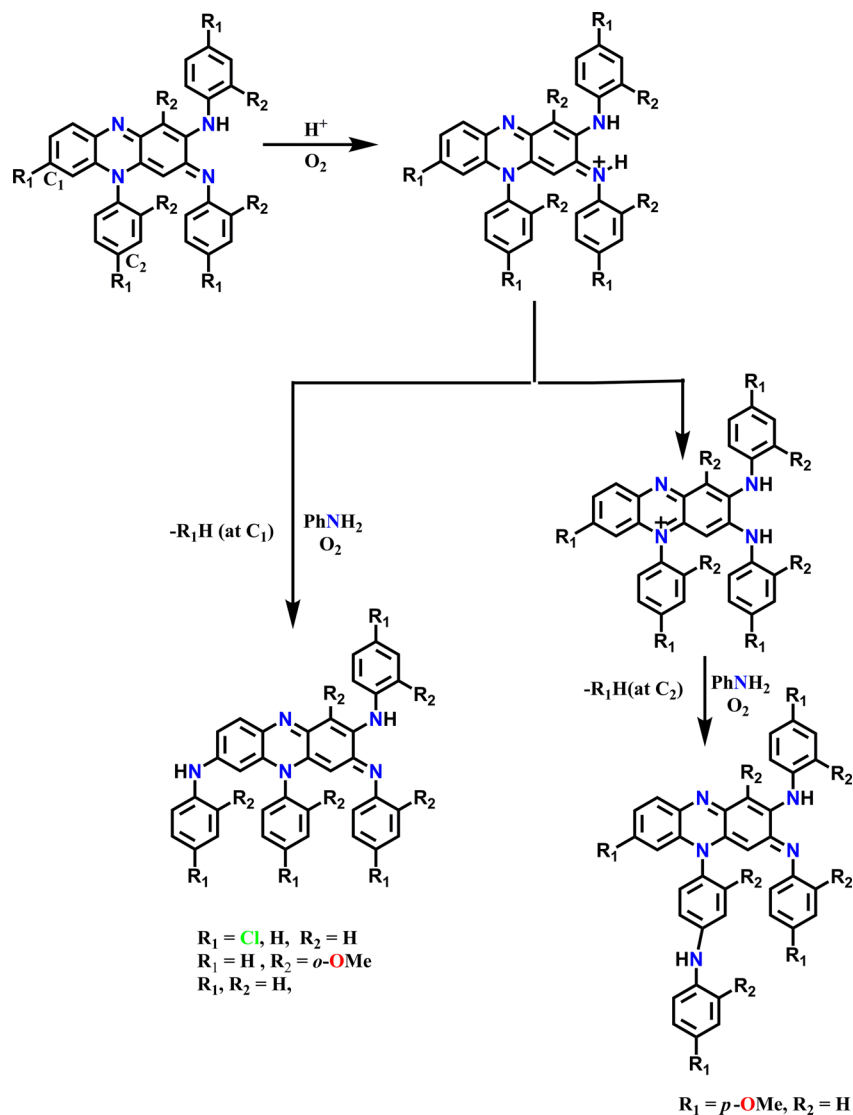
Plausible Reaction Steps. Since we have not been able to identify or isolate the intermediates of the above reactions, their mechanisms are not fully understood. However, a few general comments on the above transformations may be worthwhile. First the above reactions do not occur under anaerobic conditions, confirming that the above proton-mediated redox events are brought about by aerial oxygen. Second, the reference reactions proceed even in the presence of a radical scavenger like TEMPO (2,2,6,6-tetramethylpiperidinoxyl radical) or BHT (2,6-di-*tert*-butyl-4-methylphenol), thus excluding the involvement of radicals in the above reaction pathway. Furthermore, we note that aromatic amines are known to undergo two-electron oxidation¹⁰ under acidic conditions and the yields and rates of the reactions in the present cases are dependent¹¹ on the oxidation potentials of the amines. For example, *p*-anisidine has the least¹¹ oxidation potential (0.250 V) among the chosen primary amines and, accordingly, the corresponding phenazine (**1d**) is obtained with a greater ease and in highest yield (65%). By contrast, in the case of *p*-chloro-substituted aniline ($E^\circ = 0.86$ V) the reaction is sluggish (needs more than 72 h) and the yield of the product **1b** is low (25%). Based on the available literature, we propose that the primary step for the formation of phenazine is a $2e^-$ oxidation process, $\text{ArNH}_3^+ \rightarrow \text{ArNH}^+$ (nitrinium cation),¹⁰ which subsequently undergoes a *p*-C–N bond fusion reaction producing *p*-semidine. Repetition of the above steps and deamination¹² lead to the formation of an intermediate compound A, which

on further protonation and ring closure with C–N bond formation reaction produces the reduced form of the reference phenazine B. The final products are the results of further aerial oxidation of the intermediate B. The structure of the compound **1d** is in fact a regioisomeric analogue of the compounds **1a–c**. The proposed mechanisms for the regioselectivity of amination are shown in Schemes 4 and 5. The regioselectivity of amination are controlled by the nature of substitution on the intermediate B. Thus, whereas the chloro, hydrogen, and *o*-OMe substitution direct reactivity at carbon C₁, the *p*-OMe-substituted phenazine under similar reaction conditions shows reactivity on the C₂ atom of the pendent phenyl ring (Scheme 5).

In the cases of the secondary and tertiary amines, it is proposed that protonation at the nitrogen center followed by demethylation generates CH_3^+ , which in the presence of air produces^{13a,b} HCHO. Subsequent reaction of HCHO with *N,N*-dimethylaniline forms the intermediate compound D, which under an acidic environment is transformed to the new intermediate D₁. Repetitions of the identical steps lead to the final product (Scheme 6). Synthesis of the crystal violet from *N,N*-dimethylaniline has been documented in the literature. However, the compounds **2b–d** are not available in the literature.

Formation of compound **3** from *N*-phenyl-*o*-phenylenediamine under similar reaction conditions may be explained by considering the steps as shown in Scheme 7. The following observations may be put forward in support of our proposition: (i) it is an oxidation reaction where proton assists its oxidation;

Scheme 5. Probable Mechanism of Regioisomeric Phenazines



(ii) our efforts to convert the compound dimer **E** to **3** were unsuccessful. Thus, we presume that before dimerization two semidine units combine, via deamination and C–N bond formation,^{14a,b} to produce an intermediate species **F**. Further C–N bond formation reaction on **F** with another semidine molecule associated with aerial oxidation results in the formation of the final compound **3**.

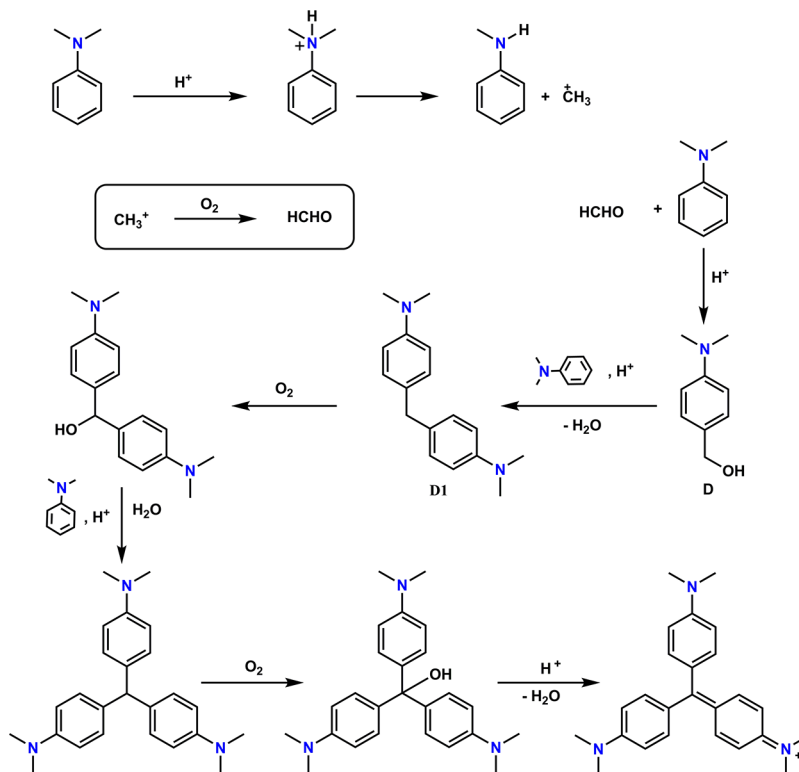
Redox Properties. Redox behavior of the newly synthesized compounds were studied by cyclic voltammetry. Detailed experimental procedures are submitted as Supporting Information. The compounds **1a–d** showed three oxidation waves along with one reduction wave. While the first oxidation process is reversible (Figure 3), the other two responses are irreversible. The irreversible redox feature is possibly due to the possibility of involvement of proton-coupled electron-transfer processes at the amine function. The redox potentials are sensitive to the nature of substitution(s) and showed parallel shift following the Hammett's substitution constants. Reversibility of the least potential oxidation wave allowed us to record the EPR spectrum of a electrogenerated cation, **1a⁺**. At low temperature (liquid nitrogen temperature), it showed a sharp EPR signal at $g = 1.998$ signifying the formation of an organic

radical (Figure 3). The one-electron oxidized compound **1a⁺** is blue (see the Figure S42, Supporting Information) and is unstable at room temperature. It readily returns to the parent compound **1a**.

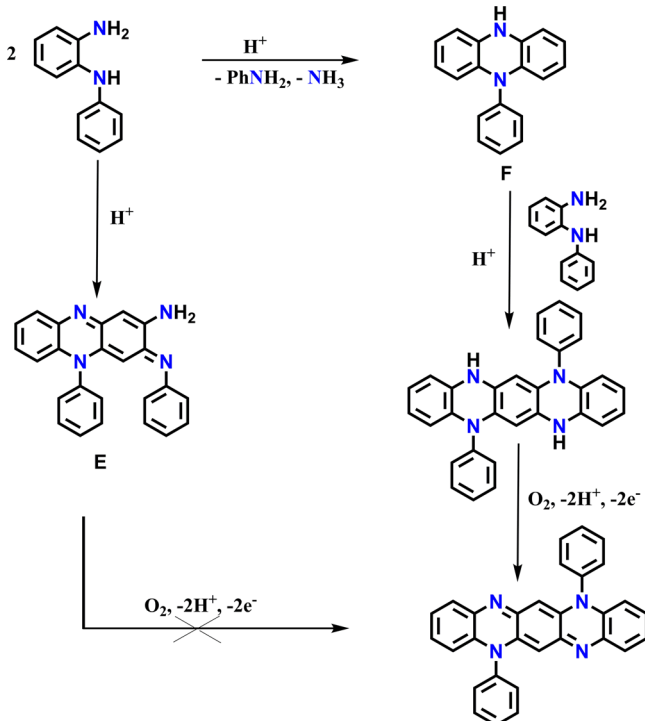
The compounds **2a–d** showed a reversible reduction and a reversible oxidation waves in the potential range -1.5 to $+1.8$ V. One-electron stoichiometry of the couples was confirmed by constant potential exhaustive electrolysis. Oxidation is believed to occur at one of the reduced amine moieties, and the reduction occurs at the oxidized *p*-quinone moiety. The pentacene-like polyaromatic heterocyclic compound **3** showed two irreversible oxidation waves and an irreversible reduction wave presumably due to oxidation of the reduced amine function and reduction for the diimine function, respectively. Electrochemical data of all the compounds have been submitted as Supporting Information, and the cyclic voltammograms of the representative compounds are available as Figures S31–S34 and Table S5 in the Supporting Information.

Spectral Properties and DFT. Spectral properties of all of the dyes were recorded in acetonitrile solvent. The spectra of the compounds **1a–d** are displayed in Figure 4, and the corresponding absorption data are collected in Table S3

Scheme 6. Probable Mechanism of Triarylmethane Dye



Scheme 7. Probable Mechanism of the Compound 3



(Supporting Information). In general, these compounds display a moderately intense broad transition in the range 475–605 nm.

The lowest energy transition in these compounds is sensitive to the donor strength of the amine residue. Thus, the chloro-substituted phenazine **1b** showed the lowest energy absorption

at 601 nm while that for **1d** (with *p*-OMe substitution) appeared at 478 nm. The compounds **1a–d** showed acidochromic properties. A representative compound **1a** was studied for this purpose. Color of the compound **1a** is bluish-violet and shows an absorption at 514 nm. Upon addition of 1 equiv of trifluoroacetic acid (TFA), an intense transition at 601 nm appeared which is associated with a shoulder at 514 nm. Gradual addition of further TFA ultimately produced an ink-blue solution. The spectral change is shown in Figure 5. Since the two sites viz. N3 and N1 are suitable for protonation, two-step processes are also evident in the spectral change. However, the compound **1e** has only one such nitrogen available for protonation and is reflected in its spectral change (see Figure S38, Supporting Information). Protonation of the amine residue triggers a strong intramolecular charge transfer between the donor amine and the acceptor quinone chromophore resulting in red shift of absorption.

Similarly, compound **3** undergoes protonation, and accordingly its purple color became blue in $[\text{H3}]^+$. X-ray structure determination has confirmed that protonation occurs at only one imine nitrogen viz. N11.

These types of compounds also showed solvatochromism. ^{15a–c} Solvatochromism of the compound **2a** has been reported, ^{16a–c} and thus, we will not discuss it further. The two representative compounds **1a** and **3** have been studied for this purpose. Their spectra were recorded in different solvents ranging from low-polar toluene to highly polar methanol. In the case of **1a**, the color change is more prominent. Its solution in toluene is red-violet and it becomes blue in methanol. Spectral changes of **1a** and **3** are shown in the Figures S35–S37, S39, and S40 (Supporting Information).

To gather information on the origin of these transitions, we analyzed the B3LYP/6-31G(d)¹⁷ optimized geometries of the compounds **1a** and **3** by DFT calculations. The bond lengths

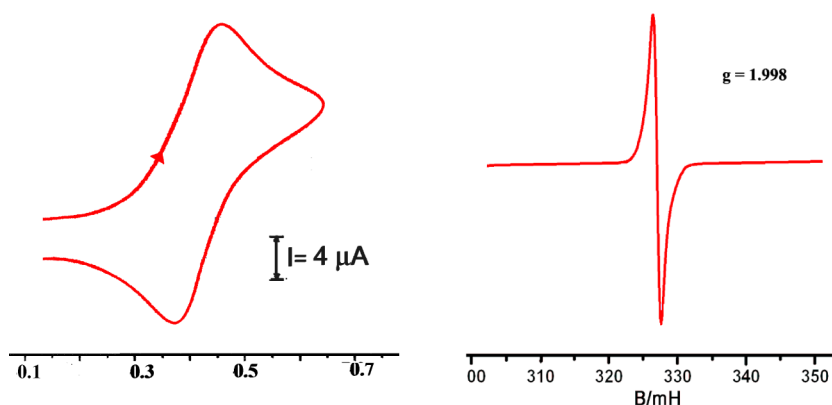


Figure 3. Cyclic voltammogram and EPR spectrum of compound 1a.

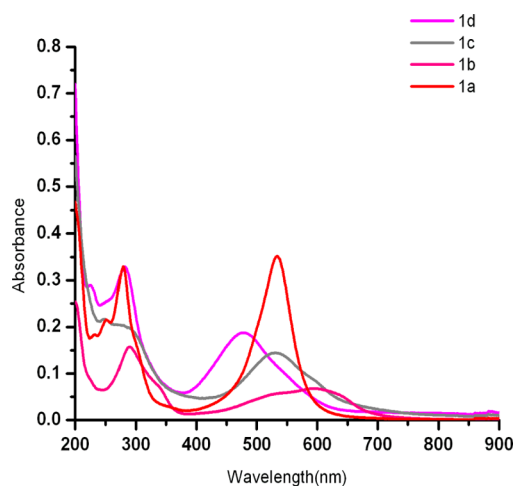


Figure 4. UV-vis spectra of 1a–1d in CH₃CN.

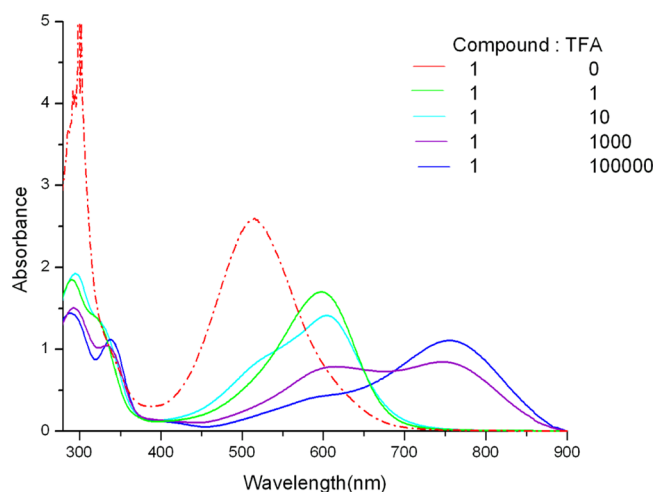


Figure 5. UV-vis spectral change of 1a upon addition of TFA in CH₂Cl₂ solution.

and bond angles of the gas-phase optimized structures match well with the experimental data (Tables 1–3).

The lowest energy transitions of the compounds, assigned using the TD-DFT analysis, match well with the experimental ones. The calculated transitions, oscillator strengths, and the experimentally observed transition are listed in Table S4 (Supporting Information). The analysis of the frontier MOs of the compound 1a indicates that the distribution of HOMO and

Table 1. Selected Bond Distances (Å) for 1a, 1d, and 1e

bond length	1a		1d		1e	
	exptl	calcd	exptl	calcd	exptl	calcd
N1–C18	1.377(5)	1.364	1.315(3)	1.318	1.322(3)	1.318
N2–C13	1.398(5)	1.391	1.375(3)	1.393	1.390(3)	1.393
N3–C15	1.371(5)	1.369	1.306(3)	1.309	1.311(3)	1.309
N4–C16	1.386(5)	1.382	1.363(3)	1.366	1.372(3)	1.366
C13–C18	1.395(6)	1.402	1.467(4)	1.470	1.464(3)	1.469
C13–C14	1.434(6)	1.428	1.364(4)	1.370	1.370(3)	1.374
C14–C15	1.436(6)	1.436	1.421(3)	1.430	1.431(3)	1.438
C15–C16	1.420(6)	1.416	1.488(4)	1.491	1.496(3)	1.493
C16–C17	1.421(6)	1.417	1.356(4)	1.360	1.365(3)	1.373
C17–C18	1.419(6)	1.429	1.420(3)	1.425	1.433(3)	1.430

Table 2. Selected Bond Distances (Å) for [2b]ClO₄

bond length	2b	
	exptl	calcd
C1–C2	1.455(5)	1.446
C2–C3	1.426(7)	1.425
C2–C7	1.435(8)	1.421
C3–C4	1.374(7)	1.376
C4–C5	1.423(8)	1.423
C5–C6	1.428(7)	1.420
C6–C7	1.362(7)	1.381
N1–C5	1.346(6)	1.357

LUMO is delocalized over the entire molecule. The HOMO is delocalized over the amine nitrogen (34%) as well as the π framework of the tricyclo moiety (47%), and the LUMO is delocalized on the amine nitrogen atom (37%) and extended over the tricyclo moiety (54%). On the basis of the values of the oscillatory strength predicted using TD-DFT, the most intense transition at 530 nm for the compound 1a is ascribed to the excitation from HOMO to LUMO which may be assigned as charge transfer, $\pi \rightarrow \pi^*$.

To have insight into the solvatochromism effect by DFT calculation, we optimized the compound 1a in three different

Table 3. Selected Bond Distances (Å) for [H3]CF₃SO₃

bond length	[H3]	
	exptl	calcd
N11–C44	1.349(8)	1.355
N18–C25	1.375(8)	1.391
C25–C44	1.458(8)	1.455
C25–C26	1.359(9)	1.376
C26–C27	1.399(9)	1.426
C27–C42	1.450(8)	1.455
C42–C43	1.383(9)	1.399
C43–C44	1.393(9)	1.395
N28–C27	1.322(9)	1.326
N35–C42	1.357(8)	1.367

solvents (toluene, acetonitrile, and methanol) using a conductor-like polarizable continuum model. The TD-DFT was done on the solvent-phase optimized geometry to see the solvent effect on the lowest energy transition. The transition follows the same trend, but the magnitude of shift of the lowest energy transition is smaller than the experimentally observed value (Figure 6).

Emission properties of all of the compounds were studied by fluorescence spectroscopy. The crystal violet dyes are generally fluorescent and showed maximum emission at 609 nm upon excitation at 570 nm in CH₃CN solvent at room temperature. However, in the cases of the substituted compounds **2c** and **2d** these appear at 594 and 611 nm in the same solvent. The phenazine compounds **1a–c** are nonemissive. However, their close analogue **3** exhibits strong fluorescence in CHCl₃ solvent at room temperature. The emission spectrum is structured and showed maximum emission λ_{em} in the range of 590–640 nm upon excitation at 520 nm. Notably, both the emission and absorption bands of the compound **3** are sensitive to acids. Thus, upon protonation with HCl its maximum emission λ_{em} and excitation wavelengths are red-shifted to 650–700 and 584 nm respectively.

The emission and absorption spectra of compounds **3** and [H3]⁺ are shown in Figure 7. Compound **3** was characterized by a good fluorescent quantum efficiency of 0.52, and its lifetime is 2.12 ns in CHCl₃ solvents. Notably, these values are comparable to the emission properties¹⁸ of Rhodamine 6G.

Conclusion. In summary, we have disclosed here a novel synthesis of a variety of nitrogen-containing dyes by simple acid-promoted oxidation of aromatic amines. An unusual ring-closure reaction occurs in primary aromatic amine leading to the formation of phenazines (**1a–e**) via multiple *p*-C–N bond fusion. Some of these phenazines undergo further substitution-controlled regiospecific C–N bond fusion reactions (**1a–d**). Similar reactions of *N*-phenyl-*o*-phenylenediamine provide azaacenes (**3**) as the major product and phenazine (**E**) as a minor product. In contrast, metal-mediated oxidations of aniline^{5a–k} mostly result in *o*-semidine or its higher homologues. Thus, the results of proton-catalyzed oxidation of primary aromatic amines clearly are different from transition-metal template-directed oxidation reaction. Secondary and tertiary amines react in different ways and provide triaryl-methane dyes via para carbon–carbon bond formation reaction. Notably, such a simple synthetic protocol for the synthesis of a variety of such dyes is not available in the literature. Many of the polycyclic compounds, reported herein, are new, and their single-crystal X-ray structures have been solved. Moreover, phenazines are generally biologically active aromatic natural products, and continual discoveries of new phenazine natural products indicate that a large resource of metabolites with biological significance like antibiotic, antitumor, antimalaria, and antiparasitic¹⁹ activities are still to be disclosed in Nature. Furthermore, the triphenylmethane dyes belong to an important class of commercial dyes that have been extensively employed in the medical and related biological sciences.²⁰ Polycyclic aromatic hydrocarbons like azaacene are promising for functional materials and act as n-type conducting materials for organic field effect transistor (OFET) devices.²¹ The search for practical applications of these materials is underway.

EXPERIMENTAL SECTION

Materials and Measurements. All of the reagents and chemicals were purchased from commercial sources and used without further purifications. Syntheses of the compounds were done in open atmosphere. CAUTION: Perchlorate salts of the compounds have to be handled with care and appropriate safety precautions.

¹H and ¹³C NMR spectra were recorded on a 300 or 500 MHz spectrometer, and SiMe₄ was used as the internal standard. An elemental analyzer was used to collect microanalytical data (C, H, N). ESI mass spectra were recorded on a mass spectrometer. Electronic

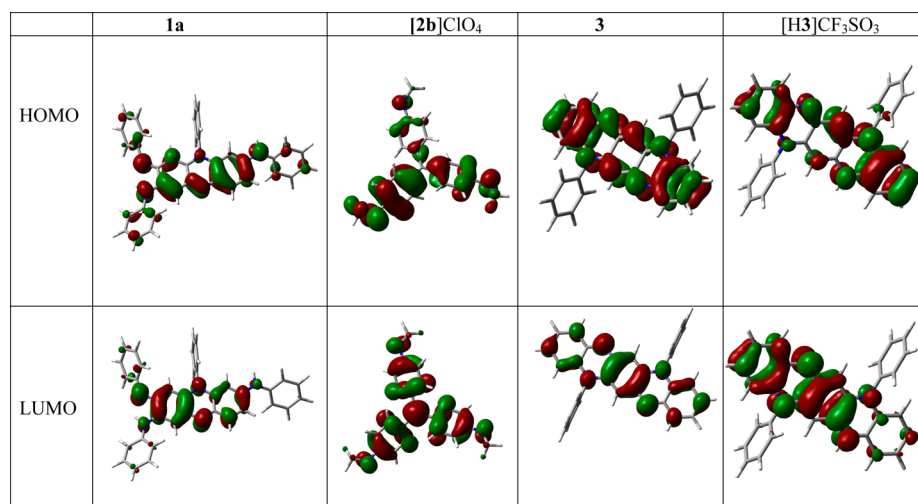


Figure 6. Electronic distributions observed for the frontier molecular orbitals of the compounds **1a**, [**2b**]ClO₄, **3**, and [H3]CF₃SO₃.

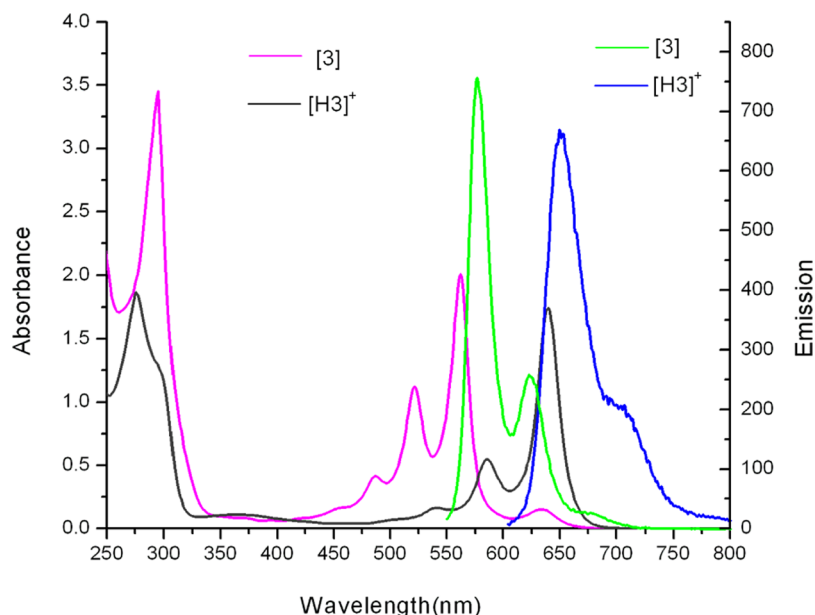


Figure 7. UV-vis and fluorescence spectra of 3 and $[H3]^+$.

absorption spectra were measured on a spectrometer using the acetonitrile solutions. Emission spectra were recorded using a spectrofluorimeter operating at room temperature (32 °C). Emission quantum yields were obtained by using rhodamin-6 ($\Phi_F = 0.78$ in ethanol) as reference. Cyclic voltammetry experiments were performed using an electrochemical analyzer with a conventional three-electrode configuration consisting of a glassy carbon working electrode, platinum auxiliary electrode, and a nonaqueous $Ag/AgNO_3$ reference electrode. The $E_{1/2}$ values were determined as $1/2(E_{pa} + E_{pc})$, where E_{pa} and E_{pc} are the anodic and cathodic peak potentials, respectively. All potentials reported are not corrected for the junction potential. The solvent in all experiments was CH_3CN , and the supporting electrolyte was 0.1 M tetraethylammonium perchlorate.

Synthesis of Phenazine Derivatives (1a–e). These compounds were synthesized by the following general procedure. A mixture of the amine (1 g) with $HClO_4$ (1 M) at 100 °C in air for 1–3 days produced substituted phenazines compound as the major products. The initial light yellow solution became dark during this period.

After being cooled to room temperature, the mixture was cleaned with diethyl ether. A dark mass thus obtained was purified on a preparative silica TLC plate using the solvent mixture toluene/chloroform/acetonitrile as eluant. The yields and spectral characterization of the products are as follows:

N2,N7,5-Triphenyl-3-(phenylimino)-3,5-dihydrophenazine-2,7-diamine (1a). Yield: 30% (284 mg). Mp: 218–220 °C. 1H NMR (300 MHz, $CDCl_3$): δ 8.35 (s, NH), 7.63 (d, 1H, $J = 8.7$), 7.54 (d, 2H, $J_1 = 7.5$), 7.43–7.38 (m, 5H), 7.27–7.10 (m, 8H), 7.01–6.93 (m, 5H), 6.83 (d, 2H, $J = 7.8$), 6.12 (s, 1H), 5.92 (s, NH), 5.44 (s, 1H). ^{13}C NMR (75 MHz, $CDCl_3$): δ 141.1 (C), 140.4 (C), 137.3 (C), 133.1 (C), 130.9 (CH), 129.7 (CH), 129.4 (CH), 128.8 (CH), 128.3 (CH), 123.1 (CH), 122.6 (CH), 121.5 (CH), 121.4 (CH), 119.3 (CH), 91.5 (C). IR (KBr, cm^{-1}): 2923, 1627, 1523, 1245, 620. ESI-MS: m/z 530 $[M + H]^+$. Anal. Calcd for $C_{36}H_{27}N_5$: C, 81.64; H, 5.14; N, 13.22. Found: C, 81.63; H, 5.15; N, 13.24.

N2,N7,5-Tris(4-chlorophenyl)-3-(4-chlorophenylimino)-3,5-dihydrophenazine-2,7-diamine (1b). Yield: 25% (218 mg). Mp: 186–187 °C. 1H NMR (500 MHz, $DMSO-d_6$): 8.82 (s, 1H), 8.58 (s, NH), 7.74 (d, 2H, $J = 8.5$), 7.61 (d, 1H, $J = 8.5$), 7.51–7.44 (m, 6H), 7.24 (t, 4H, $J = 7.5$), 7.06–7.02 (m, 3H), 6.91 (s, 1H), 6.78 (d, 2H, $J = 8.5$), 6.12 (s, 1H), 5.19 (s, NH). ^{13}C NMR (125 MHz, d_6 DMSO): δ 151.7 (C), 145.8 (C), 144.5 (C), 142.2 (C), 139.1 (C), 139.0 (C), 136.0 (C), 135.6 (C), 133.7 (C), 132.5 (C), 132.1 (C), 132.0 (CH), 131.7 (C), 131.1 (CH), 130.6 (C), 130.4 (CH), 129.9 (CH), 128.4 (CH), 127.9 (CH), 127.0 (C), 126.9 (CH), 126.7 (CH), 126.1 (CH),

124.4 (CH), 124.0 (CH), 123.9 (CH), 123.6 (CH), 121.5 (CH), 115.4 (CH), 102.5 (C), 96.3 (CH), 90.6 (CH). IR (KBr, cm^{-1}): 2910, 1590, 1523, 1228, 620. ESI-MS: m/z 668 $[M + H]^+$. Anal. Calcd for $C_{36}H_{23}N_5Cl_4$: C, 64.79; H, 3.47; N, 10.49; Cl, 21.25. Found: C, 64.7; H, 3.50; N, 10.31; Cl, 21.36.

1-Methoxy-N2,N7,5-tris(2-methoxyphenyl)-3-(2-methoxyphenylimino)-3,5-dihydrophenazine-2,7-diamine (1c). Yield: 55% (506 mg). Mp: 160–161 °C. 1H NMR (300 MHz, $CDCl_3$): δ 8.63 (s, NH), 7.73–7.70 (m, 1H), 7.37 (dd, 1H, $J_1 = 7.34$, $J_2 = 8.25$), 7.26 (s, 2H), 7.17 (d, 1H, $J = 7.39$), 7.11 (d, 1H, $J = 7.6$), 7.02–6.97 (m, 4H), 6.91–6.88 (m, 4H), 6.85–6.74 (m, 3H), 6.49 (s, 1H), 5.85 (s, 1H), 5.17 (s, NH), (3.98, 3.85, 3.81, 3.67, 3.63) ($-OCH_3$). ^{13}C NMR (75 MHz, $CDCl_3$): δ 156.1 (C), 155.3 (C), 153.9 (C), 151.2 (C), 150.8 (C), 148.8 (C), 146.7 (C), 142.9 (C), 142.0 (C), 140.8 (C), 134.2 (C), 133.6 (C), 131.3 (C), 130.2 (CH), 129.9 (CH), 125.7 (C), 121.9 (CH), 116.1 (CH), 112.9 (CH), 110.7 (CH), 101.8 (CH), 95.4 (CH), 93.9 (CH), 91.8 (CH), 56.4–55.6 (OCH_3). IR (KBr, cm^{-1}): 2927, 1629, 1526, 1240, 620. ESI-MS: m/z 680 $[M + H]^+$. Anal. Calcd for $C_{41}H_{37}N_5O_5$: C, 72.44; H, 5.49; N, 10.30; O, 11.77. Found: C, 72.43; H, 5.48; N, 10.31; O, 11.76.

7-Methoxy-N-(4-methoxyphenyl)-5-(4-(4-methoxyphenyl-amino)phenyl)-3-(4-methoxyphenylimino)-3,5-dihydrophenazine-2-amine (1d). Yield: 65% (570 mg). Mp: 175–177 °C. 1H NMR (300 MHz, $CDCl_3$): δ 8.10 (s, NH), 7.64 (d, 1H, $J = 8.82$), 7.29 (t, 3H, $J = 9$), 7.1–7.04 (m, 5H), 6.92 (d, 3H, $J = 8.91$), 6.82–6.72 (m, 7H), 6.05 (s, 1H), 5.52 (s, 1H), 4.53 (s, NH). ^{13}C NMR (75 MHz, $CDCl_3$): δ 156.2 (C), 155.3 (C), 151.2 (C), 150.9 (C), 134.2 (C), 130.2 (C), 129.9 (C), 129.2 (C), 128.4 (C), 125.8 (C), 125.4 (C), 123.6 (CH), 122.7 (CH), 122.0 (CH), 121.9 (CH), 120.9 (CH), 120.7 (CH), 120.3 (CH), 113.0 (CH), 112.1 (CH), 110.8 (CH), 102.1 (CH), 95.5 (CH), 93.8 (CH), 91.9 (CH), 56.5–55.7 (OCH_3). IR (KBr, cm^{-1}): 2930, 1650, 1535, 1235, 620. ESI-MS: m/z 650 $[M + H]^+$. Anal. Calcd for $C_{34}H_{30}N_4O_4$: C, 73.54; H, 5.01; N, 15.46; O, 11.46. Found: C, 73.43; H, 5.10; N, 15.31; O, 11.36.

7-Methoxy-N,5-bis(4-methoxyphenyl)-3-(4-methoxyphenylimino)-3,5-dihydrophenazine-2-amine (1e). Yield: 30% (225 mg). Mp: 138–140 °C. 1H NMR (300 MHz, $CDCl_3$): δ 8.10 (s, NH), 7.64 (d, 1H, $J = 8.86$), 7.32 (d, 2H, $J = 8.86$), 7.14–7.01 (m, 4H), 6.92 (d, 2H, $J = 8.89$), 6.82–6.72 (m, 6H), 6.05 (s, 1H), 5.52 (s, 1H), (3.87, 3.83, 3.77, 3.67) ($-OCH_3$). ^{13}C NMR (75 MHz, $CDCl_3$): δ 160.1 (C), 159.3 (C), 156.4 (C), 155.9 (C), 152.5 (C), 148.7 (C), 144.6 (C), 135.4 (C), 133.1 (C), 132.9 (C), 131.3 (CH), 129.9 (CH), 129.6 (CH), 129.4 (CH), 124.4 (CH), 122.6 (CH), 116.2 (CH), 114.7 (CH), 114.1 (CH), 110.2 (CH), 98.8 (CH), 91.4 (CH), 55.7–55.5

(-OCH₃). IR (KBr, cm⁻¹): 2923, 1645, 1520, 1245, 620. ESI-MS: *m/z* 559 [M + H]⁺. Anal. Calcd for C₃₄H₃₀N₄O₄: C, 73.10; H, 5.41; N, 10.03; O, 11.46. Found: C, 73.11; H, 5.40; O, 11.45.

These compounds were synthesized by the following general procedure. A mixture of the respective amine (1 g) with 1 M HClO₄ at 100 °C in air for 1 day produced substituted dyes containing the triphenylmethane moiety as the major product. The initial light yellow solution became a bright color during this period. After being cooled to room temperature, the mixture was cleaned with diethyl ether. The dark mass was purified on a preparative silica TLC plate using the solvent mixture chloroform/acetonitrile as eluant. The yields and spectral characterization of the products are as follows:

Tris(4-(dimethylamino)phenyl)methylium (2a). Yield: 35% (340 mg). Mp: 205–206 °C. ¹H NMR (300 MHz, CDCl₃): δ 7.26 (d, 2H, *J* = 8.5), 6.8 (d, 2H, *J* = 8.5), 3.20 (s, 6H). IR (KBr, cm⁻¹): 3360, 2918, 1585, 1172, 623, 1085. ESI-MS: *m/z* 372 [M]⁺. Anal. Calcd for C₂₃H₃₀N₃ClO₄: C, 64.25; H, 6.64; N, 8.65. Found: C, 64.26; H, 6.63; N, 8.66.

Tris(4-(methylamino)phenyl)methylium (2b). Yield: 40% (400 mg). Mp: 192–194 °C. ¹H NMR (300 MHz, CDCl₃): δ 7.7 (d, 2H, *J* = 6), 6.59 (d, 2H, *J* = 8.4), 4.71 (s, NH), 2.89 (s, 3H). ¹³C NMR (75 MHz, CDCl₃): δ 207.1 (C), 152.4 (C), 132.5 (CH), 127.6 (C), 111.0 (CH), 31.0 (CH₃). IR (KBr, cm⁻¹): 3355, 2916, 1525, 1172, 620, 1085. ESI-MS: *m/z* 330 [M]⁺. Anal. Calcd for C₂₂H₂₄N₃ClO₄: C, 62.23; H, 5.90; N, 9.47. Found: C, 62.24; H, 5.91; N, 9.45.

Tris(4-amino-3,5-diisopropylphenyl)methylium (2c). Yield: 20% (180 mg). Mp: >250 °C. ¹H NMR (300 MHz, CDCl₃): δ 7.09 (s, 2H), 5.46 (s, NH₂), 3.10–2.92 (q, 2H), 1.27 (d, 12H, *J* = 6.6). ¹³C NMR (75 MHz, CDCl₃): δ 182.0 (C), 150.9 (C), 134.8 (CH), 132.2 (C), 128.6 (C), 27.8 (CH), 22.3 (CH₃). IR (KBr, cm⁻¹): 3396, 2923, 1579, 620, 1085. ESI-MS: *m/z* 540 [M]⁺. Anal. Calcd for C₃₇H₅₄N₃ClO₄: C, 69.40; H, 8.50; N, 6.56. Found: C, 69.24; H, 8.31; N, 6.65.

Tris(4-amino-3,5-dimethylphenyl)methylium (2d). Yield: 20% (195 mg). Mp: >250 °C. ¹H NMR (500 MHz, DMSO-*d*₆): δ 6.92 (s, 2H), 6.74 (s, NH₂), 2.13 (s, 6H). ¹³C NMR (125 MHz, DMSO-*d*₆): δ 150.7 (C), 134.6 (C), 134.5 (CH), 132.1 (C), 128.6 (C), 22.7 (CH₃). IR (KBr, cm⁻¹): 3365, 2956, 1535, 620, 1085. ESI-MS: *m/z* 372 [M]⁺. Anal. Calcd for C₂₅H₃₀N₃ClO₄: C, 63.62; H, 6.41; N, 8.90; Found: C, 63.24; H, 6.80; N, 8.60.

Compounds **3** and **E** were synthesized by the following reaction between *N*-phenyl-*o*-phenylenediamine and perchloric acid at 100 °C in air for 1 day. The initial dark solution became blue during this period. After being cooled to room temperature, the mixture was cleaned with diethyl ether. The crude mass was purified on a preparative silica TLC plate using the solvent mixture chloroform as eluant. The yields and spectral characterization of the products are as follows:

5,12-Diphenyl-5,12-dihydroquinoxalino[2,3-*b*]phenazine (3). Yield: 20% (118 mg). ¹H NMR (300 MHz, CDCl₃): δ 7.61 (t, 3H, *J* = 7.2), 7.41–7.16 (m, 7H), 7.07 (t, 2H, *J* = 7.5), 6.89–6.78 (m, 6H), 5.34 (2H, s). ¹³C NMR (75 MHz, CDCl₃): δ 147.6 (C), 144.3 (C), 131.2 (C), 130.5 (CH), 127.7 (CH), 126.8 (CH), 121.1 (CH), 120.8 (CH), 117.9 (CH), 117.1 (CH). IR (KBr, cm⁻¹): 1620, 620. ESI-MS: *m/z* 437 [M + H]⁺. Anal. Calcd for C₃₀H₂₀N₄: C, 82.55; H, 4.62; N, 12.84. Found: C, 82.6; H, 4.51; N, 12.64.

3,5-Dihydro-5-phenyl-3-(phenylimino)phenazin-2-amine (E). Yield: 15% (140 mg). ¹H NMR (500 MHz, DMSO-*d*₆): δ 7.65 (d, 1H, *J* = 8), 7.59 (t, 2H, *J* = 7.5), 7.52 (t, 1H, *J* = 7.5), 7.35 (d, 2H, *J* = 7.5), 7.18–7.11 (m, 4H), 6.88 (t, 1H, *J* = 10), 6.67 (d, 2H, *J* = 8), 6.58 (s, NH), 6.44 (t, 2H, *J* = 10), 5.22 (s, 1H). IR (KBr, cm⁻¹): 2930, 1625, 1540, 1250, 620. ESI-MS: *m/z* 363 [M + H]⁺. Anal. Calcd for C₂₄H₁₈N₄: C, 79.54; H, 5.01; N, 15.46. Found: C, 79.60; H, 4.91; N, 15.40.

X-ray Crystallography. Suitable X-ray quality crystals (0.11 × 0.13 × 0.18) of [**1a**], (0.12 × 0.14 × 0.16) [**1b**], (0.12 × 0.14 × 0.16) [**1d**], (0.11 × 0.14 × 0.16) [**1e**], and (0.07 × 0.09 × 0.26) [H₃]CF₃SO₃ were obtained by slow evaporation of a dichloromethane solution of the compound, and (0.10 × 0.13 × 0.16) [**2b**]ClO₄ was obtained by slow diffusion of dichloromethane hexane mixture of the

compound. The data were collected on a Bruker SMART APEX-II equipped with graphite-monochromated Mo K α radiation (λ = 0.71073 Å) and were corrected for Lorentz polarization effects. A total of 7877 [**1a**], 11337 [**1b**], 32727 [**1d**], 27130 [**1e**], 9716 [**2b**]ClO₄, and 14604 [H₃]CF₃SO₃ reflections were collected, out of which 2509 [**1a**], 4119 [**1b**], 9235 [**1d**], 5459 [**1e**], 999 [**2b**]ClO₄, and 2240 [H₃]CF₃SO₃ were unique [*R*_{int} = 0.0472 [**1a**], 0.068 [**1b**], 0.0459 [**1d**], 0.0450 [**1e**], 0.0677 [**2b**]ClO₄ and 0.0436 [H₃]CF₃SO₃] and used in subsequent analyses. The structure was solved by employing the SHELXS-97 program package and refined by full-matrix least-squares based on *F*² (SHELXL-97). All hydrogen atoms were added in calculated positions. Crystallographic data of **1a,b,d,e**, [**2b**]ClO₄, and [H₃]CF₃SO₃ are collected in Table S1, Supporting Information.

DFT. Full geometry optimizations of the compounds were carried out using the density functional theory methods at the (R) B3LYP.¹⁷ Calculations were performed without any symmetry constraints. H, C, and N were assigned the 6-31G* basis set. All calculations were performed with the GAUSSIAN09W program package.²² The vibrational frequency calculations were performed to ensure that the optimized geometries represent the local minima and that there are only positive eigenvalues. Singlet excitation energies based on B3LYP-optimized geometries were computed using the time-dependent density functional theory (TD-DFT) formalism²³ in acetonitrile using the conductor-like polarizable continuum²⁴ model. GAUSS-SUM²⁵ was used to calculate percentage contribution of various groups to the frontier orbital and the fractional contributions of various molecular orbitals in the optical spectral transition.

■ ASSOCIATED CONTENT

● Supporting Information

X-ray crystallographic data tables for **1a,b,d,e**, [**2b**]ClO₄, and [H₃]CF₃SO₃; relevant figures for characterization. This material is available free of charge via the Internet at <http://pubs.acs.org>.

■ AUTHOR INFORMATION

Corresponding Author

*Tel: +91-33-24734971. Fax: +91-33-24732805. E-mail: icsg@iacs.res.in.

Notes

The authors declare no competing financial interest.

■ ACKNOWLEDGMENTS

Financial support received from the Department of Science and Technology (Project SR/S1/IC/0031/2010), New Delhi, is gratefully acknowledged. S.G. sincerely thanks DST for a J. C. Bose fellowship. Crystallography was performed at the DST-funded National Single Crystal Diffractometer Facility at the Department of Inorganic Chemistry, IACS. S.K.R., S.S., M.S., and P.G. are thankful to the Council of Scientific and Industrial Research for their fellowships.

■ REFERENCES

- (1) Lindsay, R. J. In *Comprehensive Organic Chemistry*; Stoddart, J. F., Ed.; Pergamon Press: New York, 1981; Vol. 2, p 165.
- (2) (a) Godula, K.; Sames, D. *Science* **2006**, *312*, 67. (b) Cho, S. H.; Kim, J. Y.; Lee, S. Y.; Chang, S. *Angew. Chem., Int. Ed.* **2009**, *48*, 9127. (c) Wolfe, J. P.; Wagaw, S.; Marcoux, J.-F.; Buchwald, S. L. *Acc. Chem. Res.* **1998**, *31*, 805. (d) Muci, A. R.; Buchwald, S. L. *Top. Curr. Chem.* **2002**, *219*, 131. (e) Surry, D. S.; Buchwald, S. L. *Angew. Chem., Int. Ed.* **2008**, *47*, 6338. (f) Phipps, R. J.; Gaunt, M. J. *Science* **2009**, *323*, 1593.
- (3) (a) Hili, R.; Yudin, A. K. *Nat. Chem. Biol.* **2006**, *2*, 284. (b) *Amino Group Chemistry, From Syntheses to the Life Science*; Ricci, A., Ed.; Wiley-VCH: Weinheim, 2007. (c) Hassan, J.; Sévignon, M.; Gozzi, C.; Schulz, E.; Lamire, M. *Chem. Rev.* **2002**, *102*, 1359.

- (4) Li, D.; Huang, J.; Kaner, R. B. *Acc. Chem. Res.* **2009**, *42*, 135 and references cited therein.
- (5) (a) Mitra, K. N.; Goswami, S. *Chem. Commun.* **1997**, 49. (b) Mitra, K. N.; Majumder, P.; Peng, S.-M.; Castiñeiras, A.; Goswami, S. *Chem. Commun.* **1997**, 1267. (c) Mitra, K. N.; Peng, S.-M.; Goswami, S. *Chem. Commun.* **1998**, 1685. (d) Ghosh, A. K.; Mitra, K. N.; Mostafa, G.; Goswami, S. *Eur. J. Inorg. Chem.* **2000**, 1961. (e) Majumder, P.; Falvello, L. R.; Tomàs, M.; Goswami, S. *Chem.—Eur. J.* **2001**, *7*, 5222. (f) Das, C.; Goswami, S. *Comments Inorg. Chem.* **2003**, *24*, 137. (g) Mitra, K. N.; Choudhury, S.; Castiñeiras, A.; Goswami, S. *J. Chem. Soc., Dalton Trans.* **1998**, 2901. (h) Mitra, K. N.; Goswami, S. *Inorg. Chem.* **1997**, *36*, 1322. (i) Samanta, S.; Adak, L.; Jana, R.; Mostafa, G.; Tuononen, H. M.; Ranu, B. C.; Goswami, S. *Inorg. Chem.* **2008**, *47*, 11062. (j) Samanta, S.; Goswami, S. *J. Am. Chem. Soc.* **2009**, *131*, 924. (k) Samanta, S.; Goswami, S. *Inorg. Chem.* **2011**, *50*, 3171.
- (6) (a) Soper, J. D.; Kaminsky, W.; Mayer, J. M. *J. Am. Chem. Soc.* **2001**, *123*, 5594. (b) Soper, J. D.; Saganic, E.; Weinberg, D.; Hrovat, D. A.; Benedict, J. B.; Kaminsky, W.; Mayer, J. M. *Inorg. Chem.* **2004**, *43*, 5804. (c) Bai, G.; Stephan, D. W. *Angew. Chem., Int. Ed.* **2007**, *46*, 1856.
- (7) Dalpozzo, R. *Chem. Rev.* **2010**, *110*, 3501.
- (8) (a) Seillan, C.; Brisset, H.; Siri, O. *Org. Lett.* **2008**, *10*, 4013. (b) Ma, Y.; Sun, Y.; Liu, Y.; Gao, J.; Chen, S.; Sun, X.; Qiu, W.; Yu, G.; Cui, G.; Hu, W.; Zhu, D. *J. Mater. Chem.* **2005**, *15*, 4894. (c) Casu, M. B.; Imperia, P.; Schrader, S.; Falk, B.; Jandke, M.; Stroehriegel, P. *Synth. Met.* **2001**, *124*, 79. (d) Jenekhe, S. A. *Macromolecules* **1991**, *24*, 1.
- (9) Tang, Q.; Liu, J.; Chan, H. S.; Miao, Q. *Chem.—Eur. J.* **2009**, *15*, 3965.
- (10) Marjanovic, C. G.; Konyushenko, N. E.; Trchova, M. S. *Synth. Met.* **2008**, *158*, 200.
- (11) Wawzonek, S.; McIntyre. *J. Electrochem. Soc.* **1967**, *114*, 1023.
- (12) Kottenhahn, A. P.; Seo, E. T.; Stone, H. W. *J. Org. Chem.* **1963**, *28*, 3114.
- (13) (a) Mao, Y.; Bakac, A. *J. Phys. Chem.* **1996**, *100*, 4219. (b) Kesavan, L. *Science* **2011**, *331*, 195.
- (14) (a) Takahashi, K.; Eguchi, H.; Shiwaku, S.; Hatta, T.; Kyoya, E.; Yonemitsu, T.; Mataka, S.; Tashiro, M. *J. Chem. Soc., Perkin Trans. 1* **1988**, 1869. (b) Tashiro, M.; Fukuda, Y.; Yamato, T. *Heterocycles* **1981**, *16*, 771.
- (15) (a) Fleischhauer, J.; Beckert, R.; Jüttke, Y.; Hornig, D.; Günther, W.; Birckner, E.; Grummt, U. W.; Görls, H. *Chem.—Eur. J.* **2012**, *18*, 4549. (b) Singh, P.; Baheti, A.; Thomas, K. R. *J. Org. Chem.* **2011**, *76*, 6134. (c) Aaron, J. J.; Maafi, M. *Spectrochim. Acta* **1995**, *51A*, 603.
- (16) (a) Lewis, L. M.; Indig, G. L. *Dyes Pigments* **2000**, *46*, 145. (b) Lueck, H. B.; McHale, J. L.; Edwards, W. D. *J. Am. Chem. Soc.* **1992**, *114*, 2342. (c) Korppi, T. J.; Yip, R. W. *Can. J. Chem.* **1981**, *59*, 191.
- (17) Lee, C.; Yang, W.; Parr, R. G. *Phys. Rev. B* **1988**, *37*, 785.
- (18) Fleischhauer, J.; Beckert, R.; Jüttke, Y.; Hornig, D.; Günther, W.; Birckner, E.; Grummt, U. W.; Görls, H. *Chem.—Eur. J.* **2009**, *15*, 12799.
- (19) Laursen, J. B.; Nielson, J. *Chem. Rev.* **2004**, *104*, 1633.
- (20) Duxbury, F. D. *Chem. Rev.* **1993**, *93*, 381.
- (21) (a) Sun, S.; Dalton, L. R. In *Introduction to Organic Electronic and Optoelectronic Materials and Devices*; CRC: London, 2008. (b) Pron, A.; Gawrys, P.; Zagorska, M.; Djurado, D.; Demadrille, R. *Chem. Soc. Rev.* **2010**, *39*, 2577. (c) Cheng, Y. J.; Yang, S. H.; Hsu, C. S. *Chem. Rev.* **2009**, *109*, 5868. (d) Celli, J. P.; Spring, B. Q.; Rizvi, I.; Evans, C. L.; Samkoe, K. S.; Verma, S.; Pogue, B. W.; Hasan, T. *Chem. Rev.* **2010**, *110*, 2795. (e) Hagfeldt, A.; Boschloo, G.; Sun, L.; Kloo, L.; Pettersson, H. *Chem. Rev.* **2010**, *110*, 6595. (f) Szacilowski, K.; Macyk, W.; Drzewiecka-Matuszek, A.; Brindell, M.; Stochel, G. *Chem. Rev.* **2005**, *105*, 2647. (g) Mishra, A.; Ma, C. Q.; Buerle, P. *Chem. Rev.* **2009**, *109*, 1141. (h) Murphy, A. R.; Frchet, J. M. J. *Chem. Rev.* **2007**, *107*, 1066. (i) Hains, A. W.; Liang, Z.; Woodhouse, M. A.; Gregg, B. A. *Chem. Rev.* **2010**, *110*, 6689. (j) Mishra, A.; Behera, R. K.; Behera, P. K.; Mishra, B. K.; Behera, G. B. *Chem. Rev.* **2000**, *100*, 1973.
- (k) Shirota, Y.; Kageyama, H. *Chem. Rev.* **2007**, *107*, 953. (l) Wu, W.; Liu, Y.; Zhu, D. *Chem. Soc. Rev.* **2010**, *39*, 1489.
- (22) Frisch, M. J.; Trucks, G. W.; Schlegel, H. B.; Scuseria, G. E.; Robb, M. A.; Cheeseman, J. R.; Scalmani, G.; Barone, V.; Mennucci, B.; Petersson, G. A.; Nakatsuji, H.; Caricato, M.; Li, X.; Hratchian, H. P.; Izmaylov, A. F.; Bloino, J.; Zheng, G.; Sonnenberg, J. L.; Hada, M.; Ehara, M.; Toyota, K.; Fukuda, R.; Hasegawa, J.; Ishida, M.; Nakajima, T.; Honda, Y.; Kitao, O.; Nakai, H.; Vreven, T.; Montgomery, J. A., Jr.; Peralta, J. E.; Ogliaro, F.; Bearpark, M.; Heyd, J. J.; Brothers, E.; Kudin, K. N.; Staroverov, V. N.; Kobayashi, R.; Normand, J.; Raghavachari, K.; Rendell, A.; Burant, J. C.; Iyengar, S. S.; Tomasi, J.; Cossi, M.; Rega, N.; Millam, N. J.; Klene, M.; Knox, J. E.; Cross, J. B.; Bakken, V.; Adamo, C.; Jaramillo, J.; Gomperts, R.; Stratmann, R. E.; Yazyev, O.; Austin, A. J.; Cammi, R.; Pomelli, C.; Ochterski, J. W.; Martin, R. L.; Morokuma, K.; Zakrzewski, V. G.; Voth, G. A.; Salvador, P.; Dannenberg, J. J.; Dapprich, S.; Daniels, A. D.; Farkas, O.; Foresman, J. B.; Ortiz, J. V.; Cioslowski, J.; Fox, D. J. *Gaussian 09*, revision A.02; Gaussian, Inc.: Wallingford, CT, 2009.
- (23) (a) Bauernschmitt, R.; Ahlrichs, R. *Chem. Phys. Lett.* **1996**, *256*, 454. (b) Stratmann, R. E.; Scuseria, G. E.; Frisch, M. J. *J. Chem. Phys.* **1998**, *109*, 8218. (c) Casida, M. E.; Jamorosi, C.; Casida, K. C.; Salahub, D. R. *J. Chem. Phys.* **1998**, *108*, 4439.
- (24) (a) Cossi, M.; Rega, N.; Scalmani, G.; Barone, V. *J. Comput. Chem.* **2003**, *24*, 669. (b) Cossi, M.; Barone, V. *J. Chem. Phys.* **2001**, *115*, 4708. (c) Barone, V.; Cossi, M. *J. Phys. Chem. A* **1998**, *102*, 1995. (d) O'Boyle, N. M.; Tenderholt, A. L.; Langner, K. M. *J. Comput. Chem.* **2008**, *29*, 839.
- (25) Leininger, T.; Nicklass, A.; Stoll, H.; Dolg, M.; Schwerdtfeger, P. *J. J. Chem. Phys.* **1996**, *105*, 1052.